Article

Advanced Control Algorithm for FADEC Systems in the Next Generation of Turbofan Engines to Minimize Emission Levels

Majid Aghasharifian Esfahani [1], Mohammadmehdi Namazi [2,*], Theoklis Nikolaidis [3] and Soheil Jafari [3]

1 School of Engineering, Science and Research Branch, Islamic Azad University, Tehran 1477893855, Iran; sharif.mjd@gmail.com
2 Department of Mechanical Engineering, Iranian Research Organization for Science and Technology (IROST), Tehran 3313193685, Iran
3 Centre for Propulsion and Thermal Power Engineering, School of Aerospace, Transport and Manufacturing (SATM), Cranfield University, Cranfield MK43 0AL, UK; t.nikolaidis@cranfield.ac.uk (T.N.); s.jafari@cranfield.ac.uk (S.J.)
* Correspondence: namazi@irost.org

Abstract: New propulsion systems in aircrafts must meet strict regulations and emission limitations. The Flightpath 2050 goals set by the Advisory Council for Aviation Research and Innovation in Europe (ACARE) include reductions of 75%, 90%, and 65% in CO_2, NO_x, and noise, respectively. These goals are not fully satisfied by marginal improvements in gas turbine technology or aircraft design. A novel control design procedure for the next generation of turbofan engines is proposed in this paper to improve Full Authority Digital Engine Control (FADEC) systems and reduce the emission levels to meet the Flightpath 2050 regulations. Hence, an Adaptive Network–based Fuzzy Inference System (ANFIS), nonlinear autoregressive network with exogenous inputs (NARX) techniques, and the block-structure Hammerstein–Wiener approach are used to develop a model for a turbofan engine. The Min–Max control structure is chosen as the most widely used practical control algorithm for gas turbine aero engines. The objective function is considered to minimize the emission level for the engine in a pre-defined maneuver while keeping the engine performance in different aspects. The Genetic Algorithm (GA) is applied to find the optimized control structure. The results confirm the effectiveness of the proposed approach in emission reduction for the next generation of turbofan engines.

Keywords: emission reduction; gas turbine aero engines; artificial neural networks; adaptive network-based fuzzy inference system

MSC: 00A69

1. Introduction

Due to the increased use of Gas Turbine Engines (GTEs) in industries such as aerospace and power generation and in power plants, improving their performance is of particular importance for different applications [1–5]. In addition to complex nonlinear systems, these engines should ensure safe and frugal operation during the flight. An important current issue for all types of gas turbine engines is reducing the emission levels.

The reduction of pollutants requires hardware and software upgrades. Various hardware improvements on engine components have been extensively investigated, including the main and secondary flow, secondary air system (SAS), bypass and core, and intake to exhaust elements [6–10]. However, pollution reduction by upgrading the control system and its software is one of the attractive and high-impact fields for gas turbine designers. A suitable software upgrade can enhance the engine performance for a variety of environmental and performance conditions thanks to the design and development flexibility of the FADEC systems. Decreasing pollution can extend the engine operational pocket in various

environmental conditions and enhance the living indices [10]. A comprehensive plan is necessary for a generalized application to industrial and aero gas turbine engines.

With the expansion of mechatronics science in recent decades, the control system of GTEs has been upgraded from fully/partly hydro-mechanical systems to fully electronic systems. and FADEC control systems are used to satisfy gas turbine engine control modes. These systems are highly effective in terms of hardware and compete in the design and optimization of the algorithm and the engine control software. The upgrade of the combustion chamber and other engine components to reduce emissions (e.g., CO, NO_x, and SN) is a costly and challenging approach in which any mistake could result in a catastrophic failure in the whole engine operation. The alternative method, however, is to modify the FADEC engine control strategy to reduce pollutant emissions by maintaining and sometimes improving the performance of the flight. The attractiveness of this approach is the minimum imposed costs that could result in the highest efficiency of reducing unintentional combustion products and maintaining the engine performance without any significant change in hardware. Hence, it is becoming increasingly popular to propose novel control algorithms for optimizing the performance and different objective functions in gas turbine aero engines. During the last two decades, several studies on the optimization of FADEC control strategy/philosophy for gas turbine engine controller gain tuning have been conducted using different methods. Fleming and his research group at the University of Sheffield started working on this approach in 1996 [11], in which they used a multi-objective Genetic Algorithm to obtain a Pareto front set of solutions for multivariable control of an engine. More results were reported on decentralized PI/PID controllers for engine control in [12,13], where applying the global optimization methods in industrial control applications was evaluated.

A novel control system can be designed by estimating the performance using engine data from previous designs. In addition to conventional methods [9,14–16], machine learning [17] has also been used to estimate the steady and transient performance of a gas turbine. Using an approach that requires less testing on a real engine to produce valid and accurate data for different engine conditions can help in designing a reliable and efficient control system. The use of optimization- and model-based controls will be more applicable for future engine control systems [18–21]. In this paper, the current FADEC logic of a real engine is redesigned and optimized with the fewest changes for a practical application.

The engine control philosophy was established based on different perspectives, e.g., decoupling the control loops [22], multivariable control [23], mean square error (MSE) objective function [24], safety considerations [25], Multi-Criteria Decision Making (MCDM) [26], and centralized and decentralized control loop gain tuning [27,28]. Performance improvement of the Min–Max control algorithm strategy has been done through several case studies and other research [28–30]. Diverse objective functions studied in the literature mentioned above focused on

- Reducing the engine response time;
- Minimizing the engine fuel consumption;
- Managing the engine constraints and physical limitations;
- Improving the pilot command tracking;
- A combination of the above objectives.

This paper, however, will focus on minimizing the emission level in gas turbine aero engines by improving the FADEC control strategy to propose a new control structure for novel civil engines to satisfy the ACARE Flightpath 2050 regulations. The ACARE set this roadmap in response to the Strategic Research Agenda (SRA) of Europe as the home to around 448 airlines and 701 commercial airports. So, the social benefit and impact of the roadmap is obvious. The Flightpath 2050 requirements are aligned with the main targets for more green and sustainable aviation. Therefore, the contribution of the paper to the knowledge in the field from the practical aspect is also obvious.

There are different aspects in aero-engine design and development that could be improved to cope with the strict limitations of the ACARE Flight Path 2050. One of the

most effective ones is the control system. The control system has a direct effect on the engine performance and operability as it deals with the fuel flow to the engine combustion chamber [31,32]. By tuning the fuel flow rate, the control system architecture and strategy will change both fuel consumption and emission levels in jet engines [33]. Therefore, recent studies have been concentrated on using optimal and hybrid control algorithms for jet engines to improve different indices in the engine performance [34,35].

For this purpose, the first step would be developing a model able to predict the emission level in the engine during different flight modes. This model should also be sufficiently quick and trustworthy to be used in the iterative optimization process. For this purpose, after generating a validated base model using commercial GTE performance modeling software, a comprehensive model will be developed using nonlinear auto-regressive approaches. Then, the controller structure will be described, and the objective functions will be defined to formulate the emission reduction procedure as an engineering optimization problem. This problem will be addressed using the Genetic Algorithm to obtain the optimized controllers for the defined objective functions. The results analysis and discussion will confirm the validity and effectiveness of the proposed approach in the design and development of an optimal controller for gas turbine engines from an emission point of view that could be considered as a potential option towards the ACARE Flightpath 2050.

2. Performance Model of the Engine

Without loss of generality, the CFM56-5a is selected as the case study in this paper. By using commercial software (GSP and Gasturb), the base model for the engine is developed to generate the steady-state and transient performance of the engine. The validity of the generated model is confirmed against publicly available data provided by the manufacturer, as shown in Table 1. In this table, FPR, BR, TIT, IMFR, F, FMFR, and SFC represent fan pressure ratio, bypass ratio, turbine inlet temperature (K), input mass flow rate (Kg/s), thrust (KN), fuel mass flow rate (Kg/s), and specific fuel consumption (Kg/Nh), respectively. In this simulation, reaching the maximum fan and core speed at the Take-Off (TO) condition is very close to the reality of the base engine. The speeds in the simulation are 102.78%, and 104.8%, respectively (of the maximum speeds); these values are 102%, and 105% of the corresponding maximum speeds mentioned in the manufacturer's catalogue. This base model will be used to generate a comprehensive model for the controller optimization procedure.

Table 1. Comparison of the engine performance characteristics between simulation software and manufacturer's catalogue (adopted from [36]).

Parameters	Design Point (CRUISE) Simulation	Design Point (CRUISE) Catalogue Data	Off-Design Point (TAKE-OFF) Simulation	Off-Design Point (TAKE-OFF) Catalogue Data
FPR	1.6	–	1.5541	1.55
BR	5.8	–	6.00033	6
TIT	1375	–	1538.15	1538.15
IMFR	151.5	–	368.86	386.85
F	22.268	22.268	111.400	344.111
FMFR	0.4	–	1.05	–
SFC	0.06121	0.0612	0.03364	0.03364

After confirming the validity of the generated model, all required parameters, including the rotational speed of low-pressure and high-pressure shafts (N1 and N2), compressor discharge pressure (P3), and emission parameters (CO, Smoke number, and NO_x), are extracted at different flight modes and operating conditions such as maximum and minimum acceleration. These comprehensive, reliable data could be used to generate a fast nonlinear model suitable for the iterative optimization procedures.

3. Comprehensive Nonlinear Engine Model

Due to the availability of the reliable engine model and the requirement to reduce the time cost, using existing direct modeling (physical thermodynamic) methods is not feasible for design and optimization. For this nonlinear system, it is better to use indirect methods such as ANFIS, LOLIMOT, cluster fuzzy, ANFIS cluster, NARX, Hammerstein–Wiener, and so on. To stimulate the comprehensive model, the Amplitude Modulated Pseudo-Random Binary Sequence (APRBS) input with excitation in all predicted and unpowered amplitudes and frequencies provides the best answer in steady and transient conditions with different bits. When the actual engine is not to be implemented, signal type and the number of these conditions and bits are not limited. Figure 1 shows how to simulate these signal steps. α, β, and λ are the maximum input, the minimum input (fuel spray rate), and the minimum settling time of the system, respectively. R is the number of input signal bits. Applying the final generated signal with bit variations, as well as the amplitude and frequency of high excitation in model, provides the necessary engine outputs for training, checking, and testing the final comprehensive model for design and optimization software.
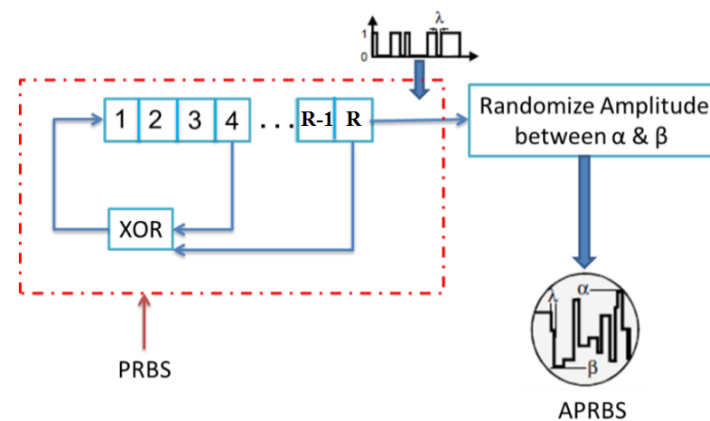
Figure 1. APRBS signal calculation steps.

To model the behavior of engine parameters, different autoregressive approaches could be taken into account. Hence, various models have been developed to study the prediction accuracy of the dynamic behavior of the engine parameters, including

- ARX (exhaustive search)
- NARX (GA optimized)
- Polynomial NARX (trial and error)
- Hammerstein–Wiener (GA optimized)
- Predicted ANFIS (sequential forward search)
- Predicted ANFIS (exhaustive search)

Based on previous and current input and output signals, SI-SO models in MATLAB can be used to predict the correlation between the turbofan input (fuel flow rate in this paper) and one of the engine parameters. In this approach, the previous input signals and engine outputs affect the following results. Moreover, the SI-SO structure is capable of using static and dynamic blocking methods. In this case, (1) auto-regressive and (2) directional blocks are applied to create gray box models. The aim of the present paper is to correlate the input fuel flow rate to engine parameters in static and dynamic flight operation modes.

Auto-regressive models can be linear or nonlinear. The linear models are generally faster. For a complex and nonlinear turbofan system, a nonlinear model or a set of linear models must be applied for different operating modes. These models have been widely used in various systems, e.g., ARX [37], NARX or Nonlinear ARX [38] in neural networks, and ANFIS [39] in adaptive neuro fuzzy application. These models consist of three main parts: regressors, nonlinear structure, and nonlinear estimator. These regressors represent the derived signals from previous input and output signals that are used as input to

ensure a dynamic model alongside a steady model. The correct choice of these regressors has a great effect on the model accuracy. The nonlinear structure determines how the regressor is placed within the linear and nonlinear layers of the F function. The F function is the nonlinear estimator that estimates the final output parameter. F can contain a variety of nonlinear functions, such as neural and fuzzy networks. The wavenet multilayer perceptron neural network is used as a nonlinear estimator in this paper. The nonlinear neuro fuzzy estimator does the same in ANFIS. As a result of its fast structure, easy optimization, estimating power, and fast learning, wavenet is more useful for estimating the F function. Hence, this structure is used in this study as a nonlinear estimator for various engine parameters. The polynomial NARX includes not only the regressors but also their exponents as additional regressors. This approach is characterized by complexity, high accuracy, and longer processing times.

To choose the regressors, different approaches were considered, e.g., exhaustive and sequential forward search, optimization, and trial and error.

The Normalized Root Mean Square Error (NRMSE) method is used as the criterion for choosing the best model for each parameter. The exact match of the parameters with the output data of the reference model shows the high accuracy of these models. To minimize NRMSE error in the modeling procedure, optimization algorithms such as genetics, "exhaustive search", and "sequential forward search" are used to calculate the design coefficients of each model. In the optimization algorithm, the maximum number of previous input and output variables (regressor) of the engine and the delay in inputs are calculated. All of the maximum past regressors are contributed to the new input in the model (m, n, d). In this case, the transient output of each moment is obtained from $y(t) = g\left(u^{t-n}, y^{t-m}\right) + v(t)$, where y is the desired output, g is a function of input variables at different times, v is a function of time, and t is the time. By determining the linear and nonlinear estimation functions through the neural network and also the parameters m, n, and d by error optimization, it would be possible to provide the best prediction output at any given moment. m, n, and d are the number of previous outputs, the number of past input signals, and the input delay, respectively. These parameters (m, n, d) are specified from the error optimization algorithm to determine the number of previous signals and input delay in the model to predict the future output.

All past system regressors up to m and n of the previous signal are applied in ARX and NARX. If a model with acceptable accuracy is obtained by trial and error, there is no need for the time-consuming optimization process. For this reason, the optimization method is not generally applicable. Optimization of NARX model parameters (m, n, d) takes more than twelve hours. The required time varies for different parameters. The optimization time is much longer for Polynomial NARX.

In the "exhaustive search", the combination of all input constants with the previous transponders of the transient model are applied, and the best ones are selected.

In the "sequential forward search", the first regressor is selected, which is the best answer for minimizing the error. The second regressor contains the best combination with the first selection, and the third is the best combination with the first two, and this process is continued. The use of "exhaustive search" or even "sequential forward search" is only applicable for very high-speed models.

A number of regressors are selected for the exhaustive and sequential forward search methods. In the present study, ten regressors u(k − 1), u(k − 2), . . . , u(k − 6) and y(k − 1), y(k − 2), y(k − 3), y(k − 4) were considered, in which u, y, k represent input, output, and the current sample index, respectively. In the exhaustive search method, all three combinations of expressed regressors are examined for training data, and the combination with the minimum error is chosen. The sequential forward search method begins by selecting the regressor with the lowest error. Its binary combination with other regressors is then evaluated for the least error to choose the second regressor. The third and final regressor is then chosen so it has the least error when combined with the other two regressors selected in the previous step. An exhaustive and sequential forward search method has been used

in both ANFIS and ARX models. The trial and error or optimization for the NARX and polynomial NARX models can be applied.

The directional block models include dynamic linear and static nonlinear blocks. The block direction and their combinations make Wiener, Hammerstein, Hammerstein–Wiener, and Wiener–Hammerstein models. For the turbofan engine in the present study, the Hammerstein–Wiener model was chosen, which had the best results for predicting pollutants. More details about the Hammerstein–Wiener model are provided in [40]. The Ten Piece-Wise Linearization function is applied for the static nonlinear part. The parameters (nb, nf, nk) are number of zeros plus one, number of poles, and input delay, respectively.

The polynomial NARX was used wherever NARX, Hammerstein–Wiener, ANFIS, and ARX models did not have the accuracy and feasibility for implementation. The model speed was drastically decreased as a result.

Table 2 shows the results of the final NRMSE test of various models for different engine output parameters, where N1, N2, P3, NO_x, CO, and SN are normalized fan speed, normalized core speed, normalized static pressure at the inlet of the combustion chamber, normalized nitrogen x-oxide, normalized carbon monoxide, and normalized smoke number, respectively. An underline indicates the model with the lowest NRMSE.

Table 2. Comparing errors in different models based on the normalized root mean square of the normalized NRMSE error.

Model	N1	N2	P3	NO_x	CO	SN
ARX (Exhaustive Search)	0.0564	0.073	0.022	0.032	0.067	0.103
NARX (GA Optimized)	0.00014	0.000112	0.000147	<u>0.000153</u>	0.0434	0.0071
Polynomial NARX (Trial and Error)	<u>0.00002</u>	<u>0.000011</u>	<u>0.000062</u>	–	–	–
Hammerstein–Wiener (GA Optimized)	0.00026	0.000691	0.000311	0.000302	0.0147	<u>0.000197</u>
Predicted ANFIS (Sequential Forward Search)	0.00017	0.0000129	0.000128	0.000196	<u>0.0005</u>	0.000255
Predicted ANFIS (Exhaustive Search)	0.00003	0.00002	0.00016	0.0002	0.0005	0.000261

The existing models in MATLAB were used in this study. To evaluate the training data, the results of GSP with APRBS signal were used. The test results of the model with an APRBS signal are shown in Table 3.

Table 3. The test results of the model with a APRBS signal.

| Engine Parameters	Chosen Model	Model Parameters	NRMSE
N1	NARX	(1, 1, 1)	0.000142
N2	NARX	(1, 1, 0)	0.000112
P3	NARX	(1, 5, 3)	0.000147
CO	ANFIS	Regressors: CO(k−1), CO(k−2), Wf(k−5)	0.0005
NOx	NARX	(2, 5, 1)	0.000153
SN	Hammerstein–Wiener	(16, 13, 1)	0.000197

It is better to have a smaller error in the models for performance parameters N1, N2, and P3, since they are crucial in accurate design and optimization of the controller, especially in achieving mechanical limitations. The NARX model indicated better results than other models for these parameters. Hence, Polynomial NARX was used to increase the accuracy. The results are shown in Table 4. It should be noted that due to the time-consuming optimization process, trial and error was used to determine its parameters.

Table 4. The parameters used in Polynomial NARX.

Engine Parameters	Polynomial Power	Model Parameters	NRMSE
N1	3	(1, 1, 0)	0.00002
N2	4	(1, 1, 0)	0.000011
P3	5	(1, 1, 0)	0.000062

Based on the values of the errors for different parameters listed in Tables 2–4, the best model for each parameter was selected. The final model architecture with the minimum error is shown in Figure 2.
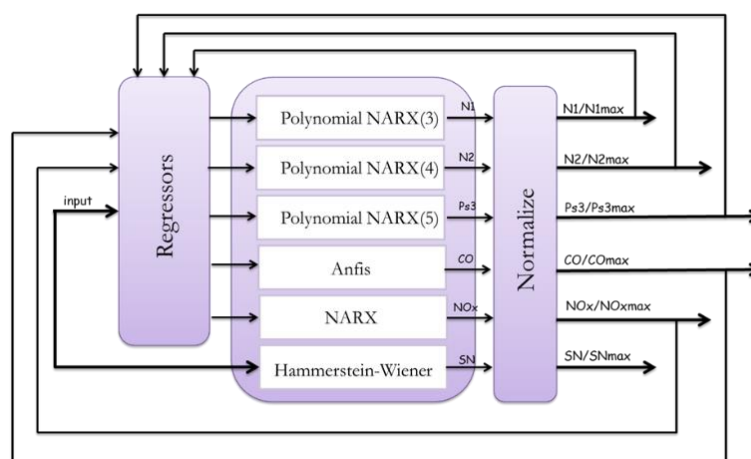
Figure 2. Turbofan engine final model.

In the design and optimization (Figure 2), input is the amount of fuel flow rate (Wf). In addition to u, the inputs to the auto-regressive model contain regressors of both input u and output (including turbofan gas turbine parameters).

4. Turbofan Engine Controller Optimization

The main objective of the gas turbine engine controller is to provide the thrust level according to the pilot's command while keeping the fuel flow within the operating range. The control of the turbofan engine includes primary and accessory control loops, with a pre-defined Min–Max selection strategy to choose the best control loop at each instantaneous time for the engine. The detailed design procedure of this controller is presented within the BRITE/Euram project OBIDICOTE (On Board Identification, DIagnosis and COntrol of gas Turbine Engines) and confirmed by all OBIDICOTE partners (SNECMA, Rolls–Royce plc, MTU Aero Engines, Volvo Aero Corporation, Fiat Avio, Techspace Aero S.A., Lufthansa Technik AG, Aerospatiale, Chalmers University of Technology AB, National Technical University of Athens, Technische Universität München, Universität Stuttgart, and Université Catholique de Louvain). Hence, this scheme is a pragmatic control technique for gas turbine engines [41–43].

This industrial controller includes separate control loops:

- Steady-state control loop, in which the steady-state fuel flow is calculated based on the engine operating condition;
- Transient control loop, in which the engine acceleration and deceleration is controlled regarding the power lever angle (PLA);
- Physical limitation control loops, in which the engine constraints including the engine stall, flameout, over-speed, and over-temperature limitations are controlled.

A schematic of the control structure for GTEs is shown in Figure 3. Each control loop contains PI/PID controllers to calculate the fuel flow based on the sensor values

obtained from the engine parameters [30]. To optimize the performance of the controller and the engine, the control loop gains should be tuned simultaneously based on a pre-defined objective function. The gain tuning procedure for the Min–Max controller is described in detail in [28]. The controller gains are adjusted to enhance the steady-state and transient behavior of the engine by reducing the fuel consumption and the response time of the engine.
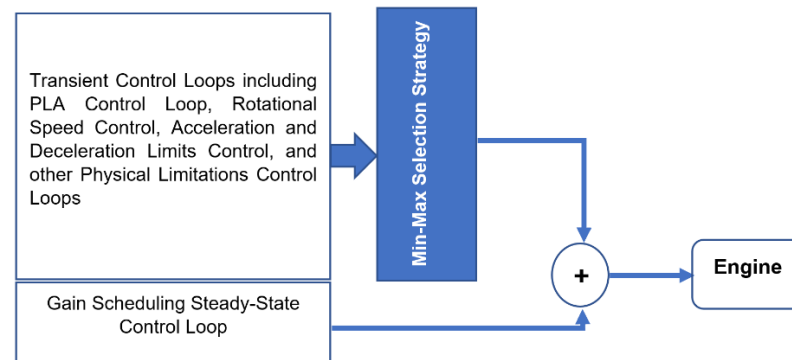

Figure 3. Schematic of engine fuel controller with Min–Max strategy (adopted from [30]).

The generated model in this paper is capable of predicting the emission level of the engine. Hence, emission reduction can be set as the objective function for the controller gain tuning procedure. An alternative method is to add the emission control strategy as a new loop in the engine controller structure. Nevertheless, the latter method would be costly for both engine designers and manufacturers. It also requires a long process of certification and reliability testing. Therefore, the optimization procedure in this paper will focus on gain tuning of the Min–Max control algorithm to minimize the emission level of the engine.

To compare the results with other optimization aspects, different objective functions are defined and considered as follows:

- J_a: Maneuverability criteria (Reducing the time of transient changes);
- J_b: Tracking criteria (Reducing the steady-state error and over/undershoot);
- J_c: Fuel burn criteria (Reducing the specific fuel consumption);
- J_d: Emission level (Reducing pollutant emissions generated during the journey).

Moreover, the engine constraints (over-speed, over-temperature, surge, etc.) are considered as penalty functions $p(x)$. The mathematical expression of J_a, J_b, J_c, and J_d are presented in Equations (1)–(4). The relation of penalties is extracted from the Yokota, Gen, Ida, and Taguchi method [44], which is used in the nonlinear planning problem and is presented in Equation (5).

$$J_a = \frac{\sum_{i=1}^{n} ts(i)}{sim_{time}}, \tag{1}$$

$$J_b = \sum_{i=1}^{n} (MP(i) + SSE(i)), \tag{2}$$

$$J_c = \int_0^{sim_{time}} \frac{\dot{m}_f}{\left\{\dot{m}_f\right\}_{max} \times \frac{sim_{time}}{sample_{time}}} dt, \tag{3}$$

$$J_d = \frac{NO_x(u)}{norm(1)} + \frac{CO(u)}{norm(2)} + \frac{SN(u)}{norm(3)}, \tag{4}$$

$$p(x) = 1 + \frac{1}{m} \sum_{i=1}^{m} \left(\frac{\Delta b_i(x)}{b_i}\right)^{\alpha}, \quad \Delta b_i(x) = Max\{0, g_i(x) - b_i\}. \tag{5}$$

In Equations (1)–(4), n is the number of changes in the requested speed (thrust) by the pilot in the input, ts is the time the engine needs to reach 98% of the requested speed

by the pilot (tolerance of two percent error), *MP* is over/undershoot of command, *SSE* is steady-state error, $\dot{m}_f$ is discharge amount of fuel input to the engine at any moment, $\{\dot{m}_f\}_{max}$ is the maximum amount of fuel discharge, sim_{time} is simulation time, $sample_{time}$ is the simulation time step, *t* is time, and *u* is the engine setting in the optimization target. $\Delta b_i(x)$ is the value of violation of the constraint m. Finally, the objective function is defined as in Equation (6).

$$J = (\beta_1 \times J_a + \beta_2 \times J_b + \beta_3 \times J_c + \beta_4 \times J_d) \times \prod P_j. \tag{6}$$

In Equation (6), β_i values represent the significance of each function, and P_j values are the penalties that are violated from the allowable limits of the engine physical parameters. As all parts of the objective function are normalized in Equations (1)–(4), the summation of β_i values is equal to one.

The parameters used in the optimization method (GA) are listed in Table 5.

Table 5. The parameters used in optimization method (GA).

Parameters	Value
Population Size	42
Selection Method	Tournament (4)
Elite Count	2
Crossover Method	Scatter
Crossover Probability	0.2
Mutation Probability	0.03
Stopping Criteria	Generation = 120

5. Results

Several scenarios can be considered for the optimization of the engine pollutants. Since the controller is checked in Idle, Take-Off, Cruise, and also in acc/deceleration modes, the entire amount of the pollutants is evaluated. In this article, the three optimization approaches are taken into account as follows:

- Scenario I "initial total opt. controller": In this scenario, the objective function of Equation (6) is minimized without considering the emission part (J_d). This is to replicate the performance optimization in the literature and to obtain an initial optimized controller by considering all objectives except emission.
- Scenario II "total emission opt.": In this scenario, the objective function of Equation (6) is minimized with equal weights for all parts of the objective function. This scenario considers the emission level as a part of the objective function while keeping the optimal engine performance.
- Scenario III "emissions opt.": This scenario is similar to scenario II. However, the weighting is applied for J_d to decrease all elements of emission simultaneously. In other words, this scenario is a detailed optimization of emissions in the GTE while maintaining the optimal engine performance.
- In terms of ACARE Flight Path 2050, scenario I replicates the state-of-the-art for aero-engines. In other words, the results obtained from scenario I represents the current status of the aircraft engine control. Scenario II considers the emission level reduction as requested in the flight path 2050. Therefore, scenario II suggests the initial changes to the current control system to approach the ACARE requirements (short-term solution). Finally, in scenario III, the importance of the emission reduction is increased to approach the ACARE requirements faster (mid-term solution).

The optimization problem is addressed using the Genetic Algorithm (GA), where the parameters of the GA are set based on [45]. By applying the GA on each scenario, an optimized controller will be obtained. Thus, there are three optimized controllers for the three defined scenarios. These controllers are simulated with the engine model developed

in the previous section, and the results of the engine performance with the optimized controllers are analyzed in this section.

Figure 4 investigates the tracking ability of the optimized controllers and the satisfaction with the physical limitations. The red line shows the Thrust Lever Angle (TLA), which is the pilot command to the engine. As can be seen in Figure 4, all three optimized scenarios track the command smoothly and without error as far as they do not exceed the engine limitations (maximum permissible rotational speed in black and minimum permissible rotational speed in blue).
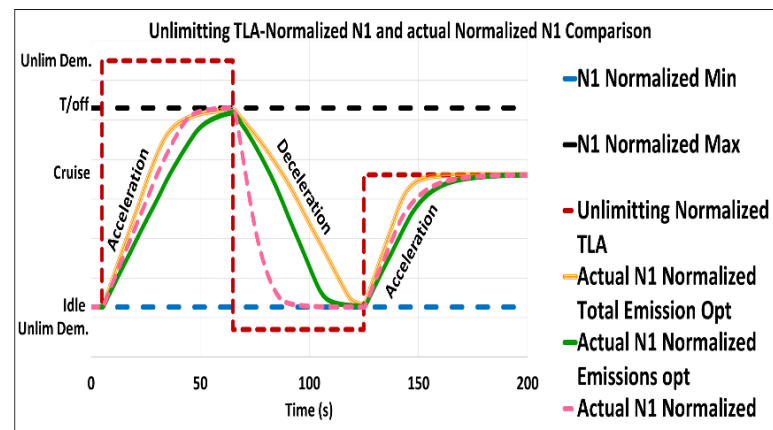
Figure 4. The tracking ability of the optimized controllers.

The emissions along the tested path are shown in Figures 5–7. According to Figure 5, in transient mode, the CO is greatly affected by the controller selection. In general, the "total emission opt." controller has the best pollution performance for the emission. The peak is in the deceleration and idle, and the "emissions opt." provides better CO pollutant performance for the engine. It is noteworthy in Figure 6 that for a NO_x pollutant, no controller for all regimes provides a specific function for the engine. In this case, for all regimes, the "total emission opt." control creates the most NO_x pollution along the path compared to the other controllers. Moreover, the "emissions opt." controller in the acceleration and the "initial total opt. controller" in the deceleration optimize the control of the exhaust NO_x. As shown in Figure 7, the SN pollutant also acts as NO_x.

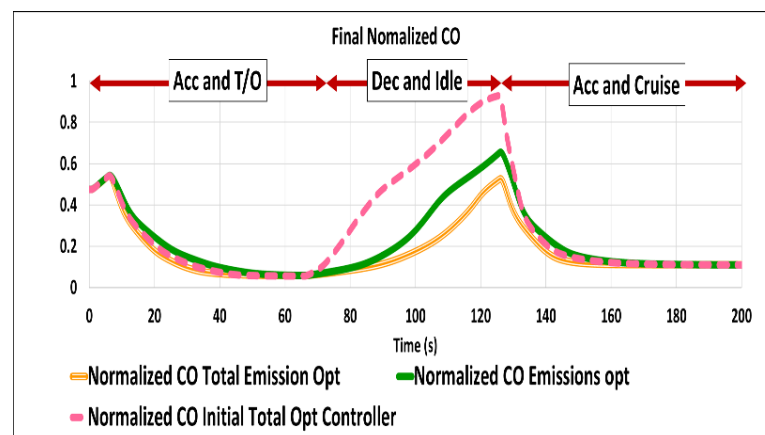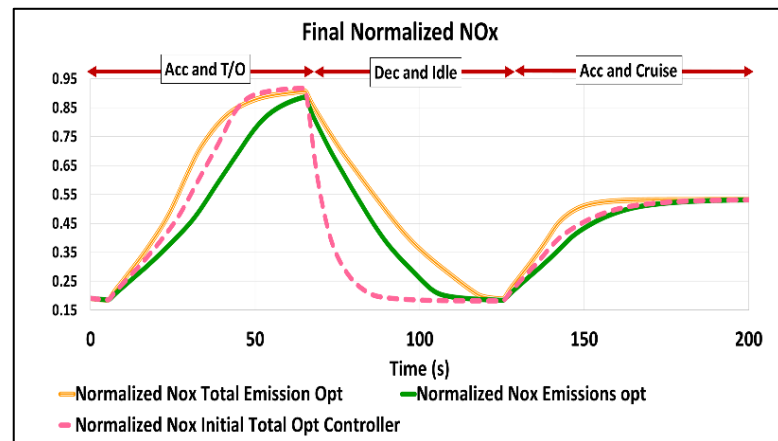**Figure 5.** CO pollutant emission of the optimized controllers.

Figure 6. NO$_x$ pollutant emission of the optimized controllers.
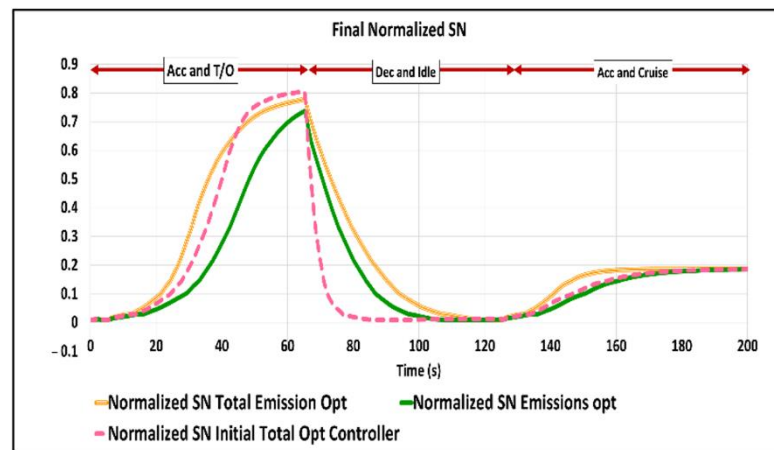

Figure 7. SN pollutant emission of the optimized controllers.

Finally, the fuel used in the combustion chamber is shown in Figure 8 for three optimized controllers. This figure shows that the "emissions opt." controller requires less fuel in transient acceleration at any time. The "initial total opt. controller" in deceleration performs the best, and the "emissions opt." is in the second rank of transient fuel consumption reduction.
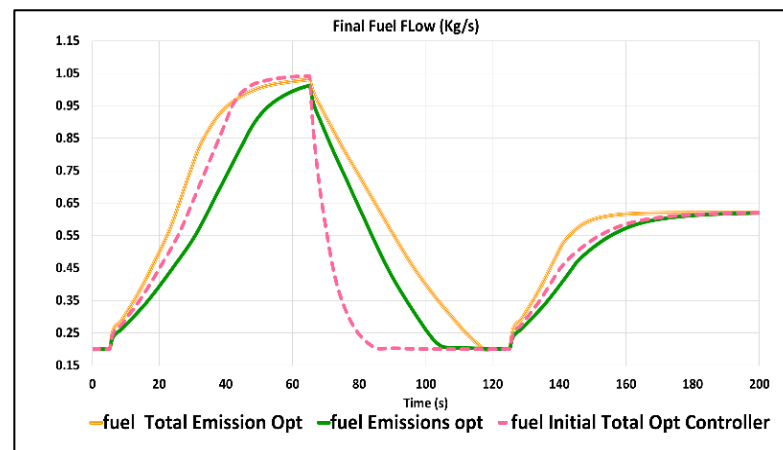

Figure 8. Fuel consumption of the optimized controllers.

6. Discussion

Pollutant analysis is essential in both steady and transient operations modes. A sudden change in fuel, especially in the deceleration, has been noted, which can exacerbate the pollutants. The CO-pollutant, which is more significant in the lower thrusts, has a high sensitivity to fuel changes. The amount of NO_x and SN pollutants increase when increasing thrusts, and their peak is in the maximum thrust, at the TO condition. Due to the low sensitivity of NO_x and SN pollutants to transient changes and their dependence on steady conditions of performance parameters such as fuel, their changes through fuel control are not high. These changes are different for the CO level. CO is more sensitive in the lower thrust, where the amount and type of fuel and air mixing affect the flame and pollutant production in combustion. This means that it is more sensitive in the lower thrust than higher thrust values. Typically, the current technology of combustion chamber designs is such that a high thrust leads to a complete burning of the fuel, which ultimately has a lower effect on transient variations. Hence, the optimal pollutant levels, especially for CO in low-power steady-state operations and deceleration transient conditions, are critical when designing and optimizing the fuel controller to reduce pollutant emissions in total. All these cases are valuable when performance is maintained, and the other design requirements are satisfied. That is why this paper focuses on four aspects of optimization (J_a to J_d) simultaneously. Figure 9 and Table 6 show the status of contaminants versus essential performance parameters for different controllers, where
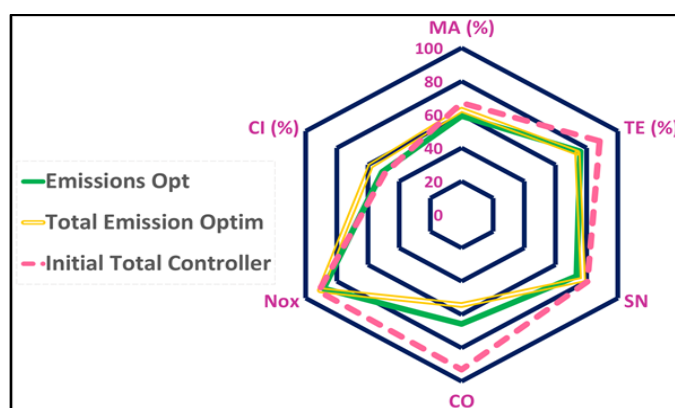

Figure 9. Comparison of three control scenarios in performance and pollution.

Table 6. Comparison of three control scenarios in performance and pollution.

Scenario	MA (%Max)	Cl (%Max)	NOx (%Max)	CO (%Max)	SN (%Max)	TE (%Max)
Initial Total Opt. Controller	66.89	49.48	91.76	93.00	80.45	88.40
Emissions Opt.	59.21	51.07	88.66	65.48	73.60	75.91
Total Emission Opt.	62.81	58.47	90.65	54.12	77.79	74.18

- MA is the percentage of maximum maneuverability (transient ability index). It is calculated into the function of maximum acc/deceleration at any moment in flight.
- The CI Index is cost relative to when the flight is at the highest level of fuel consumption at any moment (fuel consumption index).
- CO, NO_x, and SN are the corresponding pollutants relative to their maximums (CO, NO_x, and SN indices).
- TE is the average of the maximum amount of pollutants in the journey relative to the average maximum emission at any moment during the flight (average pollutant index).

Maximally expressed concepts are rarely accessible, meaning that reaching 100% of is far from reachable, and the concept of maximum is seen as a definition to compare

different scenarios together. As can be seen, the "emissions opt." is better than the other controllers in terms of optimizing all of the contaminants in different regimes and the performance, simultaneously. By using the "total emission opt.", in addition to a lower total amount of pollutants, CO has a more significant reduction (about 40%). However, these two controllers are compared to the "initial total opt. controller", and the engine performance with the "emissions opt." changes modestly. The average variation in total contaminants shows an improvement of about 15% using the proposed method in this study. The operation is carried out by the controller with changing the slope of the required changes in the transient state.

Pollutants also are calculated in different flight modes, and the results are reported in Table 7. The investigated engine is in idle mode for about ten minutes in each journey, which makes it reasonable to reduce its pollutant emissions, especially CO (as it is in low-power mode). The engine spends most of its mission in the cruise mode. In general, the fuel control system does not have much flexibility to reduce emissions in this mode. In the TO mode, NO_x and SN have good changes. Thus, it could be concluded that there is a high potential for reducing the emission level with the designed and proposed controller, especially in Idle and Take-Off modes.

Table 7. Comparison of three control scenarios in performance and pollution in different flight modes.

Scenario	T/O CO (%Max)	Idle CO (%Max)	Cruise CO (%Max)	T/O NOx (%Max)	Idle NOx (%Max)	Cruise NOx (%Max)	T/O SN (%Max)	Idle SN (%Max)	Cruise SN (%Max)
Initial Total Opt. Controller	5.61	92.72	10.98	91.76	18.19	53.14	80.43	1.21	18.55
Emissions Opt.	5.87	64.06	10.99	88.60	18.40	53.11	73.46	1.05	18.51
Total Emission Opt.	5.70	51.54	10.95	90.63	18.89	53.20	77.74	0.83	18.61

7. Conclusions

The role of the fuel controller optimization in transient changes to achieve optimal pollutant behavior in different flight modes is evaluated. CO, NO_x, and SN emission levels in steady-state and transient working conditions and various flight modes are evaluated to study how effective the optimized controller is in decreasing pollutants and satisfying the ACARE Flightpath 2050 regulations. The objective functions are considered, and three different scenarios are suggested to obtain environmentally friendly optimized controllers. The results confirm that the CO level is susceptible to fuel variation, especially in lower thrusts. The highest level of CO is in the idle mode. High CO flexibility in the face of transient variations creates a better and easier optimization potential for this parameter, especially in idle and deceleration modes. Three optimal control scenarios results are compared together to assess the engine performance. The optimized controller manages to reduce the CO level by slowing down the changes in the fuel flow rate. The "total emission opt." scenario leads to the best performance among the three defined scenarios. It enhances CO emissions by about 30% and performs well for other pollutants. The NO_x and SN pollutants are higher in the maximum thrust at Take-Off conditions. These pollutants are almost constant in the "total emission opt." controller; however, the "emissions opt." scenario performs well to improve these levels. It could be concluded that combining the optimized scenarios will result in better performance indices from an emissions level point of view. An idea for the future study would be modifying the controller setting at various flight modes based on the results of this paper to obtain the best emission performance in the whole mission.

References

1. Luo, X.J.; Fong, K.F. Control optimization of combined cooling and power system with prime mover of solid oxide fuel cell–gas turbine for building application. *Energy Procedia* **2017**, *105*, 1883–1888. [CrossRef]
2. Zamotorin, R.; Kurz, R.; Zhang, D.; Lubomirsky, M.; Brun, K. Control optimization for multiple gas turbine driven compressors. In Proceedings of the ASME Turbo Expo 2018: Turbomachinery Technical Conference and Exposition, Oslo, Norway, 11–15 June 2018. [CrossRef]
3. Nannarone, A.; Klein, S.A. Start–up optimization of a CCGT power station using model–based gas turbine control. *J. Eng. Gas Turbines Power* **2019**, *141*, 041018. [CrossRef]
4. Park, Y.K.; Moon, S.W.; Kim, T.-S. Advanced Control to Improve the Ramp-Rate of a Gas Turbine: Optimization of Control Schedule. *Energies* **2021**, *14*, 8024. [CrossRef]
5. Kim, H.R.; Kim, T.S. Optimization of Sizing and Operation Strategy of Distributed Generation System Based on a Gas Turbine and Renewable Energy. *Energies* **2021**, *14*, 8448. [CrossRef]
6. Nourin, F.N.; Ryoichi, S.A. Review of gas turbine internal cooling improvement technology. *J. Energy Resour. Technol.* **2020**, *143*, 080801. [CrossRef]
7. Inozemtsev, A.; Petrochenkov, A.; Kazantsev, V.; Shmidt, I.; Sazhenkov, A.; Dadenkov, D.; Gribkov, I.; Ivanov, P. The fuzzy logic in the problems of test control of a bypass turbojet engine gas generator. *Mathematics* **2022**, *10*, 484. [CrossRef]
8. Gao, Q.; Zhu, Y.; Liu, J. Dynamics modelling and control of a novel fuel metering valve actuated by two binary-coded digital valve arrays. *Machines* **2022**, *10*, 55. [CrossRef]
9. Yin, F.; Rao, A.G. Off-design performance of an interstage turbine burner turbofan engine. *J. Eng. Gas Turbines Power* **2017**, *139*, 082603. [CrossRef]
10. Nemitallah, M.A.; Haque, M.D.; Hussain, M.; Abdelhafez, A.; Habib, M.A. Stratified and hydrogen combustion techniques for higher turndown and lower emissions in gas turbines. *J. Energy Resour. Technol.* **2021**, *144*, JERT-21-1706. [CrossRef]
11. Chipperfield, A.; Fleming, P. Multiobjective gas turbine engine controller design using genetic algorithms. *IEEE Trans. Ind. Electron.* **1996**, *43*, 583–587. [CrossRef]
12. Tavakoli, S.; Griffin, I.; Fleming, P.J. Tuning of decentralized PI (PID) controllers for TITO processes. *Control Eng. Pract.* **2006**, *14*, 1069–1080. [CrossRef]
13. Tavakoli, S.; Griffin, I.; Fleming, P.J. Decentralized PI control of a Rolls–Royce jet engine. In Proceedings of the 2005 IEEE Conference on Control Applications, Kyoto, Japan, 28–31 August 2005. [CrossRef]
14. Li, G.; Hao, B.; Dong, J. Fault simulation and function verification of the aero-engine control system based on hardware in loop. In Proceedings of the 33rd Chinese Control and Decision Conference (CCDC), Kunming, China, 22–24 May 2021. [CrossRef]
15. Wei, Z.; Zhang, S.; Jafari, S.; Nikolaidis, T. Gas turbine aero-engines real time on-board modelling: A review, research challenges, and exploring the future. *Prog. Aerosp. Sci.* **2020**, *121*, 100693. [CrossRef]
16. Aygun, H.; Sheikhi, M.R.; Kirmizi, M. Parametric study on exergy and NOx metrics of turbofan engine under different design variables. *J. Energy Resour. Technol.* **2021**, *144*, 062303. [CrossRef]
17. Atasoy, V.E.; Suzer, A.E.; Ekici, S. A comparative analysis of exhaust gas temperature based on machine learning models for aviation applications. *J. Energy Resour. Technol.* **2022**, *144*, 082101. [CrossRef]
18. Wang, J.; Hu, H.; Zhang, W.; Hu, Z. Optimization-based transient control of turbofan engines: A sequential quadratic programming approach. *Int. J. Turbo Jet-Engines*, 2021; *in-press*. [CrossRef]
19. Xin, Z.; Feng, L.; Wenxiang, Z.; Jinquan, H. An improved multivariable generalized predictive control algorithm for direct performance control of gas turbine engine. *Aerosp. Sci. Technol.* **2020**, *99*, 105576. [CrossRef]
20. Erario, M.L.; De Giorgi, M.G.; Przysowa, R. Model-based dynamic performance simulation of a microturbine using flight test data. *Aerospace* **2022**, *9*, 60. [CrossRef]
21. Panov, V. Model-based control and diagnostic techniques for operational improvements of gas turbine engines. In Proceedings of the 10th European Turbomachinery Conference, Lappeenranta, Finland, 15–19 April 2013. [CrossRef]
22. Hwa, K.D. Neuro–fuzzy tuning of PID controller for control of actual gas turbine power. In Proceedings of the IEEE International Conference on Computational Intelligence for Measurement Systems and Applications, Boston, MA, USA, 14–16 July 2004. [CrossRef]
23. Tavakoli, S. Multivariable PID Control with Application to Gas TURBINE Engines. Ph.D. Thesis, Department of Automatic Control and Systems Engineering, University of Sheffield, Sheffield, UK, 2005.

24. Oonsivilai, R.; Oonsivilai, A. Gas turbine optimal PID tuning by genetic algorithm using MSE. *World Acad. Sci. Eng. Technol. Open Sci. Index 60 Int. J. Electr. Comput. Eng.* **2011**, *5*, 257–262. [CrossRef]

25. Montazeri–Gh., M.; Safari, A.; Jafari, S. Optimization of turbojet engine fuel control system for safety consideration. In Proceedings of the 7th Conference of Iranian Aerospace Society, Tehran, Iran, 19–21 February 2008.

26. Jafari, S.; Khalaf, P.; Montazeri–Gh, M. Multi–objective meta heuristic optimization algorithm with multi criteria decision making strategy for aero–engine controller design. *Int. J. Aerosp. Sci.* **2014**, *3*, 6–17.

27. Jafari, S.; Montazeri–Gh, M. Invasive weed optimization for turbojet engine fuel controller gain tuning. *Int. J. Aerosp. Sci.* **2013**, *2*, 138–147.

28. Montazeri-Gh, M.; Jafari, S. Evolutionary optimization for gain tuning of jet engine Min–Max fuel controller. *J. Propuls. Power* **2011**, *27*, 1015–1023. [CrossRef]

29. Aghasharifian Esfahani, M.; Montazeri–Gh, M. Designing and optimizing multi–objective turbofan engine control algorithm using Min–Max method. *Int. J. Comput. Sci. Inf. Secur.* **2016**, *14*, 1040–1050.

30. Jafari, S.; Nikolaidis, T. Turbojet Engine Industrial Min–Max Controller Performance Improvement Using Fuzzy Norms. *Electronics* **2018**, *7*, 314. [CrossRef]

31. Lutambo, J.; Wang, J.; Yue, H.; Dimirovsky, G. Aircraft turbine engine control systems development: Historical Perspective. In Proceedings of the 34th Chinese Control Conference (CCC), Hangzhou, China, 28–30 July 2015. [CrossRef]

32. Jaw, L.C.; Mattingly, J.D. *Aircraft Engine Controls*; American Institute of Aeronautics and Astronautics: New York, NY, USA, 2009; ISBN 978-1-60086-705-7.

33. Moir, I.; Seabridge, A. *Engine Control Systems*; John Wiley & Sons, Ltd.: Hoboken, NJ, USA, 2008.

34. Guolian, H.; Linjuan, G.; Congzhi, H.; Jianhua, Z. Fuzzy modeling and fast model predictive control of gas turbine system. *Energy* **2020**, *200*, 117465. [CrossRef]

35. Oglah, A.A.; Mohammed, A.J. Design of an Interval Fuzzy Type-2- PID Controller for a Gas Turbine Power Plant. *Am. Sci. Res. J. Eng. Technol. Sci. (ASRJETS)* **2018**, *44*, 155–169.

36. Roux, E. *Turbofan and Turbojet Engines: Database Handbook*; Elodie Roux: Paris, France, 2007; ISBN 9782952938013.

37. Horner, M.; Pakzad, S.N.; Gulgec, N.S. Parameter Estimation of Autoregressive-Exogenous and Autoregressive Models Subject to Missing Data Using Expectation Maximization. *Front. Built Environ.* **2019**, *5*, 2297–3362. [CrossRef]

38. Sulaiman, S.F.; Rahmat, M.F.; Faudzi, A.A.M.; Osman, K. Linear and Nonlinear ARX Model for Intelligent Pneumatic Actuator Systems. *J. Teknol.* **2016**, *78*, 21–28. [CrossRef]

39. Jang, J.S.R. Input Selection for ANFIS Learning. In Proceedings of the IEEE International Fuzzy Systems 1996, New Orleans, LA, USA, 11 September 1996. [CrossRef]

40. Abbasi-Asl, R.; Khorsandi, R.; Vosooghi-Vahdat, B. Hammerstein-Wiener Model: A New Approach to the Estimation of Formal Neural Information. *Basic Clin. Neurosci.* **2012**, *3*, 45–51.

41. Kreiner, A.; Lietzau, K. *The Use of Onboard Real–Time Models for Jet Engine Control*; MTU Aero Engines: Munich, Germany, 2003.

42. Dambrosio, L.; Camporeale, S.M.; Fortunato, B. Performance of gas turbine power plants controlled by one step ahead adaptive technique. In Proceedings of the ASME Turbo Expo 2000, Munich, Germany, 8–11 May 2000. [CrossRef]

43. Van Essen, H.A.; De Lange, H.C. Nonlinear model predictive control experiments on a laboratory gas turbine installation. *J. Eng. Gas Turbines Power* **2001**, *123*, 347–352. [CrossRef]

44. Pintér, J.D. *Global Optimization: Scientific and Engineering Case Studies*; Springer Science & Business Media: Berlin, Germany, 2006.

45. Eiben, A.E.; Smit, S.K. Parameter tuning for configuring and analyzing evolutionary algorithms. *Swarm Evol. Comput.* **2011**, *1*, 19–31. [CrossRef]